

## From prethermalization to chaos in periodically driven coupled rotors

Yonathan Sadia,<sup>1,2</sup> Emanuele G. Dalla Torre,<sup>1,2</sup> and Atanu Rajak<sup>3</sup>

<sup>1</sup>*Department of Physics, Bar-Ilan University, Ramat Gan 5290002, Israel*

<sup>2</sup>*Center for Quantum Entanglement Science and Technology, Bar-Ilan University, Ramat Gan 5290002, Israel*

<sup>3</sup>*Presidency University, Kolkata, West Bengal 700073, India*

 (Received 11 September 2021; revised 10 February 2022; accepted 25 March 2022; published 3 May 2022)

Periodically driven (Floquet) systems are said to prethermalize when their energy absorption is very slow for a long time. This effect was first discovered in quantum spin models, where the heating rate is exponentially small in the ratio between the driving frequency and the spin bandwidth. Recently, it was shown that prethermalization occurs also in classical systems with an infinite bandwidth. Here, we address the open question of which small parameter controls the lifetime of the prethermal state in these systems. We show that the lifetime is controlled by the temperature of the prethermal state, which is quasiconserved when the heating is slow. We substantiate this finding in systems of periodically driven coupled rotors, by studying the dependence of the prethermal lifetime on both the initial conditions and the connectivity. This result allows us to develop a simple analytical model that describes the crossover from prethermalization to chaos in many-body classical systems.

DOI: [10.1103/PhysRevB.105.184302](https://doi.org/10.1103/PhysRevB.105.184302)

### I. INTRODUCTION

Periodic driving of isolated many-body systems can generate novel dynamical phases that do not have any static analogs. This approach, known as Floquet engineering [1–3], led to a plethora of new phases, such as Floquet topological insulators [4–14] and time crystals [15–21]. However, periodic driving also induces heating, which hinders such novel applications. The heating can be suppressed by introducing strong disorder in interacting many-body systems, thus creating many-body localized phases [22,23]. The drawback of this method is that the disorder can destroy the generic characteristics of the nonequilibrium phases. An alternative method that can be used to reduce heating is driving the systems at high frequencies, leading to a long-lived prethermal state, where the heating rate is exponentially slowed down. This phenomenon was first discovered theoretically in quantum many-body systems [24–34]. Recently, using quantum simulator [35,36] and NMR techniques [37], the existence of long-lived prethermal states at high-frequency driving has been observed in experiments. The existence of a prethermal plateau has also been observed in interacting quantum kicked rotors, realized experimentally in optical lattices [38].

A fundamental question is whether the phenomenon of Floquet prethermalization can be found in classical systems as well. The answer to this question has been given affirmatively in the recent literature [39–44]. Using canonical models of classical chaos theory [40,43] and classical driven spin chains [41,42], a quasistationary prethermal regime has been found, before heating begins. In contrast to quantum systems, where Floquet prethermalization rigorously applies to models with bounded operators, classical prethermalization occurs in systems with unbounded spectra and has a statistical nature [40,43].

The prethermal state of periodically driven classical chaotic systems can be characterized by a generalized Gibbs

ensemble (GGE) [43–45]. For example, in the case of coupled rotors, the total angular momentum is a true conserved quantity, whereas the energy is quasiconserved inside the prethermal regime. The temperature of the prethermal state can be calculated by equating the energy of the initial ensemble, with the average energy of the GGE. When the ratio between the driving frequency and the temperature is large, the heating rate is suppressed by the low probability for the GGE to satisfy the conditions of a many-body resonance [43], leading to a statistical Floquet prethermalization. In a recent work, the different dynamical regimes of the system were further characterized by considering spatiotemporal correlations [46]. In analogy to the static case [45], these correlations show a diffusive behavior inside the prethermal regime, thus supporting the quasistatic nature of the prethermal state.

In this paper, we consider the effect of initial conditions and the connectivity of the rotors on the lifetime of the prethermal states. Our main result is that the two effects act in a similar way, namely by affecting the initial energy and hence changing the temperature of the prethermal state. First, the effect of initial conditions is investigated by tuning the standard deviation of the angles of the rotors in the initial state. By studying the dependence of the lifetime of the prethermal state on the standard deviation, we establish that the lifetime depends exponentially on the inverse temperature of the prethermal state. Next, we investigate the connectivity of the rotors by considering a many-body kicked rotor model where all the rotors interact with each other. Unlike the nearest-neighbor case, we find that the kinetic energy per rotor, for fixed initial conditions, depends on the number of rotors  $N$ , and the prethermal temperature increases linearly with  $\sqrt{N}$ . Also in this case, the lifetime varies exponentially as the inverse temperature. Starting from these results, we propose an analytical ansatz that describes the universal properties of the crossover from the prethermal regime to the chaotic one.

## II. THE MODEL: COUPLED KICKED ROTORS IN ONE AND HIGHER DIMENSIONS

In this work we consider a canonical example of chaotic, classical, many-body systems, namely the coupled kicked rotors Hamiltonian [47–53]

$$H(t) = \sum_{i=1}^N \frac{p_i^2}{2} - \Delta(t) \sum_{i,j=1|i<j}^N \kappa_{i,j} \cos(\phi_i - \phi_j). \quad (1)$$

Here,  $p_i$  and  $\phi_i$  are, respectively, the angular momentum and the angle of an  $i$ th rotor and  $N$  is the total number of rotors. The system is periodically driven with delta-function kicks,  $\Delta(t) = \sum_n \delta(t - n\tau)$ , where  $\tau$  is the time period. The couplings  $\kappa_{i,j}$  correspond to the interactions between the rotors and define the kick strength. We consider two types of interactions between the rotors: (i) a one-dimensional model with nearest-neighbor coupling, where  $\kappa_{i,j} = \kappa \delta_{i,j-1}$ , and (ii) a mean-field model with all-to-all coupling, where  $\kappa_{i,j} = \kappa/\sqrt{N}$ .<sup>1</sup>

Using Hamilton's equations of motion, one obtains a discrete map of  $p_i$  and  $\phi_i$  between consecutive kicks,

$$\begin{aligned} p_i(t + \tau) &= p_i(t) - \sum_{j \neq i} \kappa_{i,j} \sin(\phi_i - \phi_j), \\ \phi_i(t + \tau) &= \phi_i(t) + p_i(t + \tau)\tau. \end{aligned} \quad (2)$$

Here, the stroboscopic time  $t$  is defined as  $t = n\tau - 0^+$ , i.e., just before an arbitrary  $n$ th kick. These equations are a many-body generalization of the Chirikov standard map [54], a system of paramount importance for the study of the transition between regular and chaotic dynamics. By rescaling  $p_i \rightarrow p_i\tau$ , one finds that the equations of motion (2) are characterized by a single dimensionless parameter,  $K = \kappa\tau$ . Hence, in what follows, we will set  $\tau = 1$  without loss of generality. As we will see, the initial conditions and the connectivity introduce additional unitless parameters that can be used to tune the prethermal regime.

Because the model (1) is nonintegrable, at long times it shows a chaotic behavior, where the kinetic energy  $E_{\text{kin},i}(t) = \langle p_i^2(t) \rangle / 2$  grows linearly with time,  $E_{\text{kin},i}(t) \approx \Gamma t$ .<sup>2</sup> The heating rate  $\Gamma$  can be estimated using the following approach: According to Eqs. (2), the momentum at time  $t$  is equal to

$$p_i(t) = p_i(0) - \sum_{n=0}^{t-1} \sum_{j \neq i} \kappa_{i,j} \sin[\phi_i(n) - \phi_j(n)]. \quad (3)$$

Now, squaring Eq. (3) and averaging over symmetric initial values of momenta with  $\langle p_i(0) \rangle = 0$ , we obtain

$$\begin{aligned} \langle p_i^2(t) \rangle &= \langle p_i^2(0) \rangle + \sum_{m,n=0}^{t-1} \sum_{j,k \neq i} \kappa_{i,j} \kappa_{i,k} \langle \sin[\phi_i(m) \\ &\quad - \phi_j(m)] \sin[\phi_i(n) - \phi_k(n)] \rangle. \end{aligned} \quad (4)$$

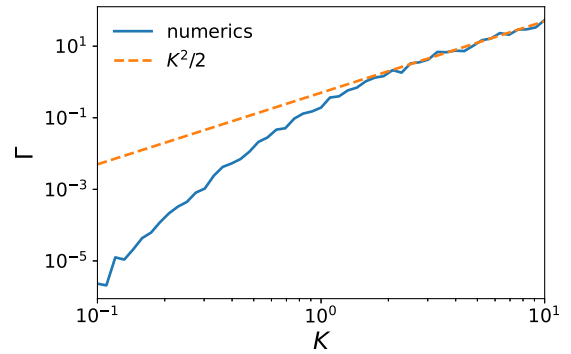


FIG. 1. Heating rate for the one-dimensional model, as a function of the coupling parameter  $K$ . For large  $K$ , it follows the relation  $K^2/2$ .

In the chaotic regime, the angles of the rotors become statistically uncorrelated both in space and time, and we can approximate  $\langle \sin[\phi_i(m) - \phi_j(m)] \sin[\phi_i(n) - \phi_k(n)] \rangle = \delta_{j,k} \delta_{m,n} / 2$ . In addition, the cross-correlation term between momenta and angles of rotors at different times can be approximated to zero, since those are uncorrelated when the time  $t$  becomes large.

For the one-dimensional model, only the terms  $j = k = i \pm 1$  contribute to the sum of Eq. (4), leading to  $\langle p_i^2(t) \rangle = K^2 t$ , or equivalently  $\Gamma = K^2/2$ . From the comparison with numerical simulations of the model, it was found that this analytical result is valid for large  $K$  only (see Fig. 1). For small  $K$ , the rotors move in a correlated way, and, for  $K \lesssim 0.1$ , the heating is approximately given by  $\Gamma \approx 10K^{6.5}$  [49,50,52]. This effect, known as “fast Arnold diffusion,” was explained in Refs. [50,55] using the concept of many-body resonance [47]. Importantly, for all values of  $K$ , the heating rate does not depend on  $N$ .<sup>3</sup>

In the case of all-to-all coupling, all terms with  $j = k \neq i$  equally contribute to Eq. (4) and one obtains  $\langle p_i^2(t) \rangle = (N-1)K^2/(2N)t$ . For large  $N$ , the heating rate,  $\Gamma \approx K^2/4$ , becomes independent of  $N$ . To verify the validity of the uncorrelated behavior of the rotors in the heating regime, we numerically compute the dynamics of the system for long times and compute the heating rate in the chaotic regime (see Fig. 2). For small values of the coupling parameter, say,  $K = 0.15, 0.3$ , we find that  $\Gamma$  increases with  $N$  and saturates to a value that is approximately given by  $K^2/8$  for large  $N$  [see Fig. 2(a)], whereas the theoretically expected value is  $K^2/4$ . This anomaly is resolved by plotting  $\Gamma$  as a function of  $K$ . From Fig. 2(b), we see that, for large  $K$  and  $N$ , the heating rate saturates to a value closer to  $K^2/4$ .

These results indicate that in both models, our assumption of an uncorrelated behavior of the angles is valid for large values of  $K$  only. For small values of  $K$  the rotors undergo a correlated dynamics, even in the diffusive long-time limit. Importantly, our simulations demonstrate that for all values of  $K$ , in both models, the heating rate does not depend on  $N$  for large enough  $N$ .

<sup>1</sup>The normalization of the latter model is discussed below.

<sup>2</sup>The heating rate  $\Gamma$  is related to the diffusion coefficient  $D$ , defined as  $\langle p_i^2 \rangle = Dt$ , by  $\Gamma = D/2$ .

<sup>3</sup>See Appendix B of Ref. [40].

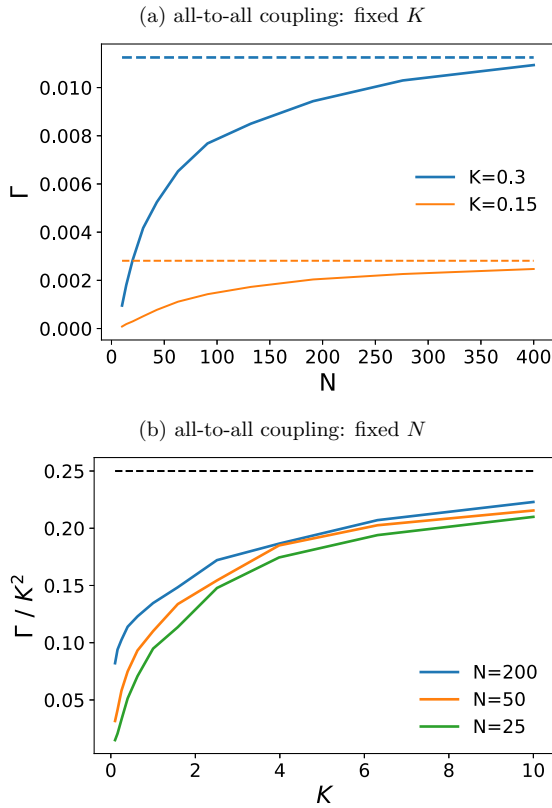


FIG. 2. (a) Heating rate as a function of  $N$  of the all-to-all coupling model for two values of  $K$ . The dashed lines correspond to  $K^2/8$ . (b) Heating rate as a function of  $K$ , for different system sizes. For large  $K$ , the heating rate tends to the mean-field value  $K^2/4$ .

### III. ENERGY AND TEMPERATURE IN THE PRETHERMAL STATE

We open our discussion by considering the prethermal regime, shortly after the initial conditions. In systems displaying statistical Floquet prethermalization, the time-averaged Hamiltonian  $H_{\text{av}}$  is quasiconserved. Here,

$$H_{\text{av}} = \frac{1}{\tau} \int_0^\tau dt H(t) = \sum_{i=1}^N \frac{p_i^2}{2} - \sum_{i,j|i<j}^N \kappa_{ij} \cos(\phi_i - \phi_j). \quad (5)$$

At short times, we can assume that the average energy in the prethermal state is equal to the average energy in the initial state

$$\langle H_{\text{av}} \rangle_T = \langle H_{\text{av}} \rangle_0, \quad (6)$$

where  $\langle \dots \rangle_T$  is the Boltzmann distribution with Hamiltonian  $H_{\text{av}}$  and temperature  $T$ , and  $\langle \dots \rangle_0$  is the average over the initial conditions. This equation can be used to derive the temperature of the prethermal state from a given set of initial conditions.

Let us first consider the one-dimensional model, where the thermal average can be performed exactly [43] and leads to

$$\frac{\langle H_{\text{av}} \rangle_T}{N} = \frac{T}{2} - K \frac{I_1(K/T)}{I_0(K/T)}. \quad (7)$$

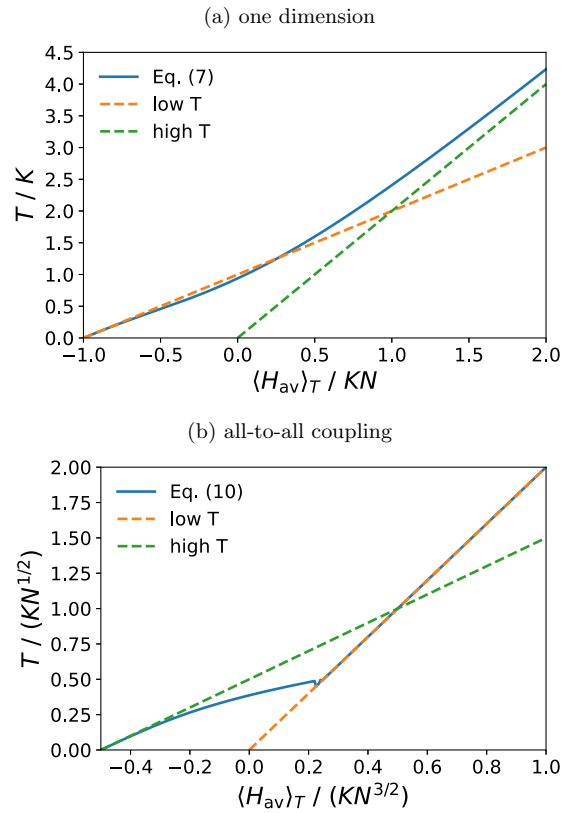


FIG. 3. Temperature as a function of the average energy  $\langle H_{\text{av}} \rangle_T$  for (a) the one-dimensional model and (b) the all-to-all coupling model, obtained by the numerical solution of Eqs. (7) and (10), respectively. The dashed lines are asymptotic results valid at small and large temperatures (see text).

Here, the right-hand side corresponds to the sum of the kinetic energy per rotor  $T/2$  and the potential energy per rotor, expressed in terms of the modified Bessel functions  $I_0$  and  $I_1$ . The numerical solution of this equation is shown in Fig. 3(a). At large temperatures,  $T \gg K$ , we can neglect the potential energy and obtain  $\langle H_{\text{av}} \rangle_T \approx NT/2$ . In the opposite limit,  $T \ll K$ , we find  $\langle H_{\text{av}} \rangle_T \approx N(T - K)$ . This result can be understood by observing that at small temperatures we can approximate  $\cos(\phi) \approx 1 - \phi^2/2$ , leading to a set of harmonic oscillators, with kinetic energy  $T/2$  and potential energy  $-K + T/2$ . The situation studied in Ref. [43] corresponds to the case  $\langle H_{\text{av}} \rangle_0 = 0$ , where  $T = 0.9384K$ .

In our numerical simulations we consider  $p_i(t=0) = 0$  and extract  $\phi_i(t=0)$  from a Gaussian distribution with standard deviation  $\sigma$ . In this case, the initial energy is

$$\frac{\langle H_{\text{av}} \rangle_0}{N} = -Ke^{-\sigma^2}. \quad (8)$$

The free parameter  $\sigma$  controls the temperature of the initial state and, consequently, the energy of the prethermal state. By equating Eqs. (8) and (7), we find an implicit relation between the parameter  $\sigma$  and the temperature of the prethermal state. In Fig. 4(a) we show that the predicted kinetic energy  $E_{\text{kin}}/N = T/2$  exactly matches the numerical solution of the model. For  $\sigma \rightarrow \infty$ , we recover the result of Ref. [43],  $T = 0.9384K$ .

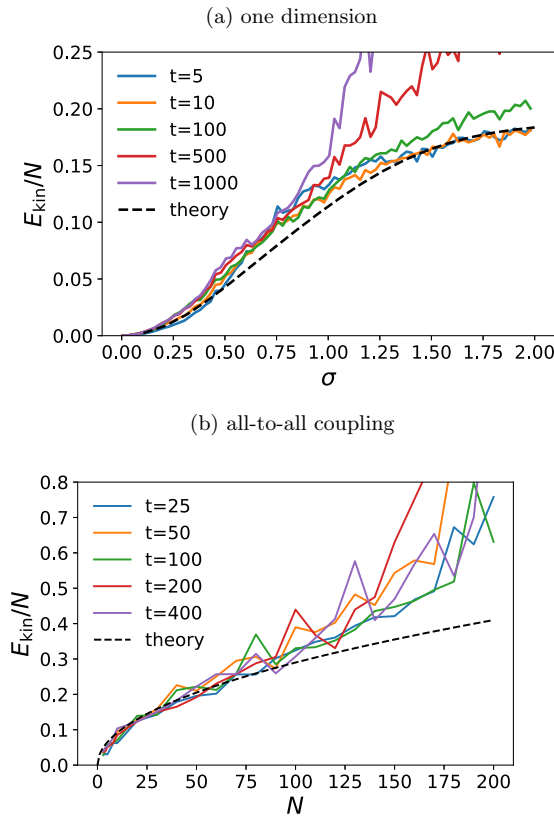


FIG. 4. Kinetic energy per rotor in the prethermal state: (a) in the one-dimensional model for  $K = 0.4$ , as a function of the initial fluctuations  $\sigma$ ; (b) in the all-to-all coupling model for  $K = 0.15$ , as a function of the number of rotors  $N$ . The dashed lines are our analytical predictions,  $E_{\text{kin}}/N = T/2$  (see text for details).

In the case of all-to-all coupling, the dependence between the energy and the temperature can be computed within a mean-field approximation [51]

$$\sum_j \cos(\phi_i - \phi_j) \approx N(\langle \cos \phi \rangle \cos \phi_i + \langle \sin \phi \rangle \sin \phi_i), \quad (9)$$

such that

$$\frac{\langle H_{\text{av}} \rangle_T}{N} \approx \frac{T}{2} - \frac{K}{2} N^{1/2} m^2, \quad (10)$$

with

$$m = \sqrt{\langle \cos \phi \rangle^2 + \langle \sin \phi \rangle^2} = \frac{I_1(c)}{I_0(c)} \quad \text{and} \quad c = \frac{K\sqrt{N}}{T} m.$$

The last line corresponds to a Boltzmann average over the Hamiltonian  $H_{\text{av}}$ , with the approximation (9). Note that Eq. (10) is a function of the rescaled parameters  $\langle H_{\text{av}} \rangle_T / (KN^{3/2})$  and  $T / (K\sqrt{N})$  only. The numerical solution of this equation is shown in Fig. 3(b). At high temperatures  $\langle \cos(\phi) \rangle = 0$ , and one simply has  $\langle H_{\text{av}} \rangle_T \approx NT/2$  (the potential energy becomes negligible). At low temperatures we find that the energy is given by  $\langle H_{\text{av}} \rangle_T = -KN^{3/2}/2 + TN$ . In our numerical simulations the rotors are initialized at random angles between 0 and  $2\pi$ , with  $p_i(t=0) = 0$ , such that the initial energy is  $\langle H_{\text{av}} \rangle_0 = 0$  and the temperature of the prethermal state is  $T = 0.3866K\sqrt{N}$  [see Fig. 4(b)]. Hence,

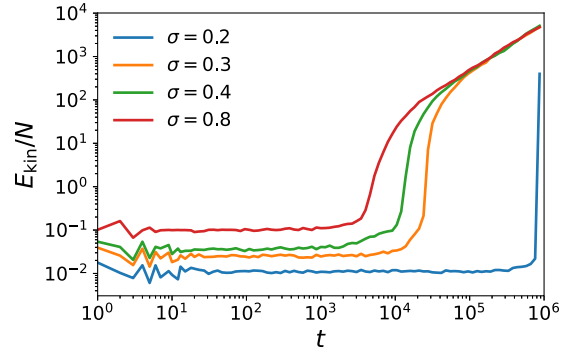


FIG. 5. Time evolution of the kinetic energy for the one-dimensional model ( $K = 0.4$ ), for different values of the standard deviation of initial angles,  $\sigma$ . As shown in Fig. 6, all the curves correspond to the same function, shifted in the time axis. The apparent change of the slope is an artifact of the logarithmic scale.

in the all-to-all coupling model the initial energy and the temperature of the prethermal state are controlled by  $N$ .

## IV. FROM PRETHERMALIZATION TO CHAOS

### A. Numerics in one dimension

We now focus on the transition between the prethermal state and the chaotic regime, starting from the one-dimensional model. Figure 5 shows the time evolution of the kinetic energy per rotor for different values of the initial fluctuations' parameter  $\sigma$ . Note that, in this plot, the transition between the prethermal and chaotic regimes appears to become sharper with decreasing  $\sigma$ . This is inconsistent with the normalization procedure proposed by Ref. [40],  $t \rightarrow t/t^*$ , which corresponds to a rigid shift in the logarithmic scale. Interestingly, we observe that the curves collapse over many orders of magnitude, when a rigid shift is applied on a linear scale,  $t \rightarrow t - t^*$ . To demonstrate this effect, in Fig. 6 we define  $t^*$  by  $E_{\text{kin}}(t^*)/N = 1$  and plot  $E_{\text{kin}}(t - t^*)/N$ , obtaining a perfect data collapse for both  $t < t^*$  and  $t > t^*$ . In Fig. 7 we show the dependence of  $t^*$  on the inverse temperature of the prethermal state and find an exponential behavior. These numerical findings will be explained by the analytical model developed in Sec. IV C.

### B. Numerics of all-to-all coupling

We now move to the case of all-to-all coupling. In Sec. II, we used a mean-field theory to compute the heating rate in the chaotic regime and demonstrated that it does not depend on the number of rotors  $N$ . In Sec. III we showed that the temperature of the prethermal state increases as  $T = 0.3866K\sqrt{N}$ . Hence, we expect that as we increase  $N$ , the lifetime of the prethermal state should decrease for a fixed value of  $K$ . This behavior is indeed observed in the numerical solution of the model (see Fig. 8). In this numerical analysis, we consider a small value of  $K$ , otherwise, the lifetime of the prethermal state will be too small to be determined by our numerics. To explore this effect in a quantitative manner, we plot the lifetime of the prethermal

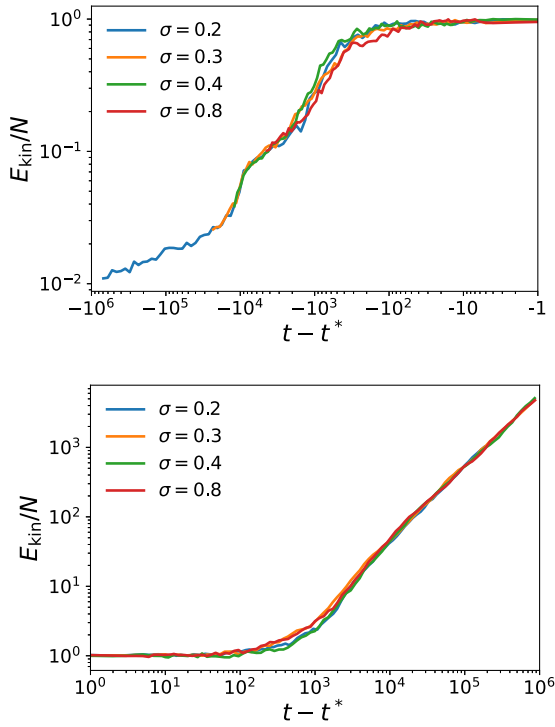


FIG. 6. Same curves as Fig. 5, for  $t < t^*$  (upper panel), and  $t > t^*$  (lower panel). The excellent data collapse demonstrates that the transition from the prethermal regime to the chaotic regime is universal and does not depend on the initial conditions.

states [defined by  $E_{\text{kin}}(t^*)/N = 1$ ], as a function of the inverse temperature, and observe two distinct regimes (see Fig. 9): (i) small inverse temperatures  $1/T < 2.5$ , corresponding to large number of rotors  $N > (0.4/0.3866K)^2 \approx 47$ ; and (ii) large inverse temperatures  $1/T > 2.5$ , corresponding to small number of rotors ( $N < 47$ ). In the former regime, the heating rate is approximately constant and we observe an exponential suppression of heating. In the latter, finite-size effects are significant (see Fig. 2) and cause a further suppression of heating.

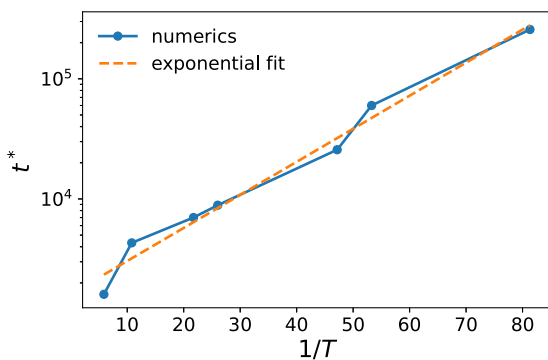


FIG. 7. Lifetime of the prethermal state of the one-dimensional model with  $K = 0.4$ , as a function of the inverse temperature of the prethermal state  $1/T$ , obtained by varying  $\sigma$ . The lifetime is exponentially large in the inverse temperature.

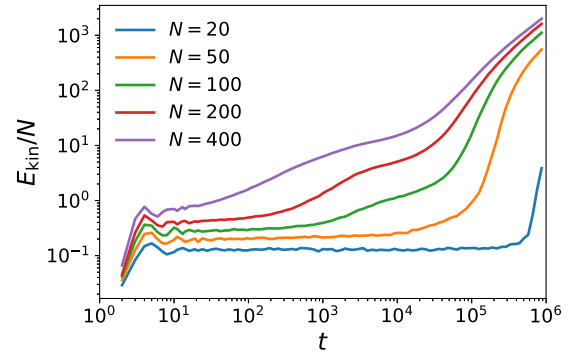


FIG. 8. Time evolution of the kinetic energy per rotor for all-to-all coupling with  $K = 0.15$ , for different values of the number of rotors  $N$ . The number of rotors affects the temperature of the prethermal state and its lifetime, while the heating rate in the chaotic regime remains constant.

### C. Effective analytic description

We now present a simple model that describes the escape from the prethermal regime to the chaotic one. The key assumption of the model is that, due to the exponentially slow absorption of energy, the prethermal state is a quasiequilibrium state, characterized by an instantaneous temperature  $T(t)$ . We consider the generic situation where the energy absorption depends exponentially on the temperature as

$$\frac{dE(t)}{dt} = N\Gamma e^{-A/T(t)}. \quad (11)$$

Here,  $\Gamma = \Gamma(K)$  is the heating rate in the high-temperature, chaotic regime, where  $dE/dt = N\Gamma$ . In models of kicked rotors, this exponential suppression of heating is due to the low probability of finding a rotor with angular momentum  $p_i \sim \Omega = 2\pi/\tau$  in a Boltzmann-Gibbs distribution with temperature  $T(t) \ll K$  [43]. See also Ref. [44] for the case of the Bose-Hubbard model, where the exponential suppression is associated to the low probability of finding sites with large occupation numbers.

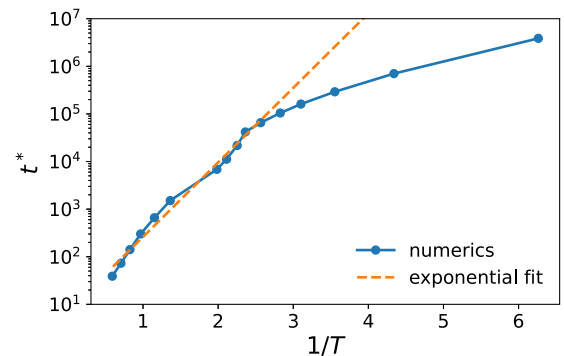


FIG. 9. Lifetime of the prethermal state for the all-to-all coupling with  $K = 0.15$ , as a function of the inverse temperature of the prethermal state. The temperature  $T$  is calculated numerically by  $T = 2E_{\text{kin}}/N$ , where  $E_{\text{kin}}$  is the kinetic energy in the prethermal state and is varied by changing  $N$  between 10 and 400. The dashed line is an exponential fit of the large temperature regime (see text).

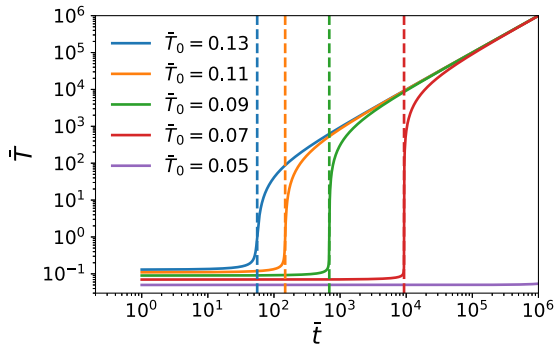


FIG. 10. Time evolution of the temperature, obtained by the numerical solution of the rescaled analytical model, Eq. (13), for different initial conditions. The dashed lines are the lifetimes of the prethermal state predicted by Eq. (15).

In order to solve Eq. (11), we need to combine it with an energy-temperature relation  $T = T(E)$ . As shown in Sec. III, this relation is often linear. For simplicity, we use here the high-temperature result  $T = 2E/N$ , such that

$$\frac{dT}{dt} = 2\Gamma e^{-A/T(t)}. \quad (12)$$

At short times,  $T(t) \approx (T_0 + 2\Gamma e^{-A/T_0}t)$  and the energy absorption is exponentially suppressed, leading to a long-lived prethermal regime. In contrast, at long times  $T(t) \approx 2\Gamma t$ , corresponding to the chaotic regime. Equation (12) offers the minimal model of statistical prethermalization, where an exponentially long prethermal regime is followed by a chaotic regime with linearly increasing temperature.

To compute the solution at intermediate times, it is useful to introduce the rescaled temperatures  $\bar{T} = T/A$  and time  $\bar{t} = 2\Gamma t/A$ , satisfying

$$\frac{d\bar{T}}{d\bar{t}} = e^{-1/\bar{T}}. \quad (13)$$

This equation has an implicit solution in terms of incomplete gamma functions, shown in Fig. 10 for different values of  $\bar{T}(0)$ . Note that all the curves are identical, up to a shift in the  $\bar{t}$  axis and the increasing sharpness for decreasing  $\bar{T}_0$  is an artifact of the logarithmic scale (see Sec. IV A).

We can evaluate the lifetime of the prethermal by computing the time at which the curve reaches some target value. This is equivalent to solving the inverse of Eq. (13), namely

$$t^* = \int_{\bar{T}_0}^1 d\bar{T} e^{1/\bar{T}}. \quad (14)$$

Here, we have set the upper limit to  $\bar{T} = 1$ , such that  $t^*$  is defined as the time required to reach  $\bar{T}(t^*) = 1$ . The integral in Eq. (14) is readily solved to deliver

$$t^* = \text{Ei}\left(\frac{1}{\bar{T}_0}\right) - \bar{T}_0 \exp\left(\frac{1}{\bar{T}_0}\right) - \text{Ei}(1) + e, \quad (15)$$

where Ei is an exponential integral function. For large  $x$ , one has  $\text{Ei}(x) \approx (1/x + 1/x^2)e^x$ , leading to

$$t^* \approx \bar{T}_0^2 \exp\left(\frac{1}{\bar{T}_0}\right). \quad (16)$$

This result shows that the lifetime of the prethermal time depends exponentially upon the inverse temperature of the state itself, as seen in our numerical solution of the one-dimensional and all-to-all coupling models.

## V. CONCLUSION

In conclusion, we performed a detailed study of the transition from prethermalization to chaos in classical periodically driven systems. We considered two tuning parameters that affect the temperature of the prethermal state, without changing the heating rate. The role of initial conditions is studied by a one-dimensional model where the temperature is set by the standard deviation of the initial Gaussian distribution of the angles. The effect of connectivity is studied in a system where all the rotors interact with each other and the temperature is a function of the number of rotors. In both cases, we computed the lifetime of the prethermal state and found that it depends exponentially on the inverse of the prethermal temperature. We repeated the same calculations in two- and three-dimensional lattices (not reported here), delivering similar results.

Starting from these numerical results, we proposed a simple model that describes the transition between prethermalization and chaos. Our model relies on two intertwined assumptions, namely that the prethermal state is fully described by its instantaneous temperature and that the heating rate is exponentially suppressed at low temperatures. The analytical solution of the resulting differential equation shows the same qualitative behavior as the numerical calculations. In particular, the lifetime of the prethermal state depends exponentially on the initial temperature of the prethermal state [see Eq. (16)]. In addition, our analytical model predicts that the curves for different initial conditions can be collapsed by a rigid shift in the time domain, as indeed observed numerically.

In this work, we considered a specific type of prethermalization, known as “statistical Floquet prethermalization.” This effect differs from a similar phenomenon that generally occurs for systems with bounded quantum operators, such as spin systems. The phenomenon of prethermalization for such systems is described by a rigorous approach, whereas our approach relies on the statistical description of the prethermal state and can be applied for a generic many-body interacting system. Another important difference between these two approaches is the dependence on the initial conditions. The rigorous approach does not depend on the initial state, whereas the statistical one depends on the initial state, through its conserved quantities.

Our work raises several questions related to the relation between statistical Floquet prethermalization and other fundamental properties of chaotic systems. The exponential scaling of the heating rate has some similarity with the phenomenon of Arnold diffusion, a characteristic of systems close to integrability. According to the Kolmogorov-Arnold-Moser (KAM) theorem, the phase space of a system close to the integrable point is almost filled with stable invariant tori. As a result, the average kinetic energy of the system is almost constant for an exponentially long time. According to the Nekhoroshev theorem, the diffusion rate is bounded by an exponential function of  $1/\epsilon^b$ , where  $\epsilon$  is the perturbation from

integrability [56]. The exponent  $b$  is inversely proportional to a polynomial function of  $N$ ; thus the diffusion rate always tends to zero as  $N \rightarrow \infty$ . Therefore, infinite systems are chaotic for any arbitrary perturbation from integrability. This is in contrast to the phenomenon of Floquet prethermalization, which survives in the limit of  $N \rightarrow \infty$ . A second key difference is that Arnold diffusion is valid in the entire phase space, while statistical prethermalization occurs only for initial conditions that correspond to low prethermal temperatures.

As mentioned in the Introduction, discrete time crystals are novel nonequilibrium phases that do not have any static analogs. These phases can be observed when the discrete time-translation symmetry of a periodically driven system is broken spontaneously. Time crystals were first predicted theoretically in driven quantum systems and later observed in experiments [17,57]. Recently, a prethermal time crystal

has been observed in a quantum simulator experiment with high-frequency drive [36]. In parallel, signatures of discrete time crystals have been found in classical systems [58,59]. An interesting question for future study is whether classical time crystals can be protected by statistical Floquet prethermalization [60,61].

## ACKNOWLEDGMENTS

We acknowledge useful discussions with Itzhack Dana and Roberta Citro. A.R. would like to thank the Department of Physics of Bar-Ilan University for computational facilities. This work was supported by the Israel Science Foundation, Grants No. 151/19 and No. 154/19. A.R. acknowledges UGC, India for Start-up Research Grant No. F. 30-509/2020(BSR).

- 
- [1] T. Oka and S. Kitamura, Floquet engineering of quantum materials, *Annu. Rev. Condens. Matter Phys.* **10**, 387 (2019).
  - [2] M. S. Rudner and N. H. Lindner, Band structure engineering and non-equilibrium dynamics in Floquet topological insulators, *Nat. Rev. Phys.* **2**, 229 (2020).
  - [3] C. Weitenberg and J. Simonet, Tailoring quantum gases by Floquet engineering, *Nat. Phys.* **17**, 1342 (2021).
  - [4] T. Oka and H. Aoki, Photovoltaic Hall effect in graphene, *Phys. Rev. B* **79**, 081406(R) (2009).
  - [5] N. H. Lindner, G. Refael, and V. Galitski, Floquet topological insulator in semiconductor quantum wells, *Nat. Phys.* **7**, 490 (2011).
  - [6] M. C. Rechtsman, J. M. Zeuner, Y. Plotnik, Y. Lumer, D. Podolsky, F. Dreisow, S. Nolte, M. Segev, and A. Szameit, Photonic Floquet topological insulators, *Nature (London)* **496**, 196 (2013).
  - [7] Y. T. Katan and D. Podolsky, Modulated Floquet Topological Insulators, *Phys. Rev. Lett.* **110**, 016802 (2013).
  - [8] G. Jotzu, M. Messer, R. Desbuquois *et al.*, Experimental realization of the topological Haldane model with ultracold fermions, *Nature (London)* **515**, 237 (2014).
  - [9] R. Fleury, A. B. Khanikaev, and A. Alu, Floquet topological insulators for sound, *Nat. Commun.* **7**, 11744 (2016).
  - [10] Y.-G. Peng, C.-Z. Qin, D.-G. Zhao *et al.*, Experimental demonstration of anomalous Floquet topological insulator for sound, *Nat. Commun.* **7**, 13368 (2016).
  - [11] R. Roy and F. Harper, Periodic table for Floquet topological insulators, *Phys. Rev. B* **96**, 155118 (2017).
  - [12] L. J. Maczewsky, J. M. Zeuner, S. Nolte *et al.*, Observation of photonic anomalous Floquet topological insulators, *Nat. Commun.* **8**, 13756 (2017).
  - [13] K. Wintersperger, C. Braun, F. N. Ünal *et al.*, Realization of an anomalous Floquet topological system with ultracold atoms, *Nat. Phys.* **16**, 1058 (2020).
  - [14] S. Mukherjee and M. C. Rechtsman, Observation of Floquet solitons in a topological bandgap, *Science* **368**, 856 (2020).
  - [15] V. Khemani, A. Lazarides, R. Moessner, and S. L. Sondhi, Phase Structure of Driven Quantum Systems, *Phys. Rev. Lett.* **116**, 250401 (2016).
  - [16] D. V. Else, B. Bauer, and C. Nayak, Floquet Time Crystals, *Phys. Rev. Lett.* **117**, 090402 (2016).
  - [17] J. Zhang, P. Hess, A. Kyprianidis *et al.*, Observation of a discrete time crystal, *Nature (London)* **543**, 217 (2017).
  - [18] N. Y. Yao, A. C. Potter, I.-D. Potirniche, and A. Vishwanath, Discrete Time Crystals: Rigidity, Criticality, and Realizations, *Phys. Rev. Lett.* **118**, 030401 (2017).
  - [19] A. Russomanno, F. Iemini, M. Dalmonte, and R. Fazio, Floquet time crystal in the Lipkin-Meshkov-Glick model, *Phys. Rev. B* **95**, 214307 (2017).
  - [20] R. Moessner and S. Sondhi, Equilibration and order in quantum Floquet matter, *Nat. Phys.* **13**, 424 (2017).
  - [21] J. Rovny, R. L. Blum, and S. E. Barrett, Observation of Discrete-Time-Crystal Signatures in an Ordered Dipolar Many-Body System, *Phys. Rev. Lett.* **120**, 180603 (2018).
  - [22] P. Ponte, Z. Papić, F. Huveneers, and D. A. Abanin, Many-Body Localization in Periodically Driven Systems, *Phys. Rev. Lett.* **114**, 140401 (2015).
  - [23] A. Lazarides, A. Das, and R. Moessner, Fate of Many-Body Localization Under Periodic Driving, *Phys. Rev. Lett.* **115**, 030402 (2015).
  - [24] S. Choudhury and E. J. Mueller, Stability of a Floquet Bose-Einstein condensate in a one-dimensional optical lattice, *Phys. Rev. A* **90**, 013621 (2014).
  - [25] M. Bukov, S. Gopalakrishnan, M. Knap, and E. Demler, Prethermal Floquet Steady States and Instabilities in the Periodically Driven, Weakly Interacting Bose-Hubbard Model, *Phys. Rev. Lett.* **115**, 205301 (2015).
  - [26] N. Goldman, J. Dalibard, M. Aidelsburger, and N. R. Cooper, Periodically driven quantum matter: The case of resonant modulations, *Phys. Rev. A* **91**, 033632 (2015).
  - [27] A. Chandran and S. L. Sondhi, Interaction-stabilized steady states in the driven  $O(N)$  model, *Phys. Rev. B* **93**, 174305 (2016).
  - [28] S. Lellouch, M. Bukov, E. Demler, and N. Goldman, Parametric Instability Rates in Periodically Driven Band Systems, *Phys. Rev. X* **7**, 021015 (2017).
  - [29] S. Lellouch and N. Goldman, Parametric instabilities in resonantly-driven Bose-Einstein condensates, *Quantum Sci. Technol.* **3**, 024011 (2018).
  - [30] D. A. Abanin, W. De Roeck, and F. Huveneers, Exponentially Slow Heating in Periodically Driven Many-Body Systems, *Phys. Rev. Lett.* **115**, 256803 (2015).

- [31] T. Kuwahara, T. Mori, and K. Saito, Floquet–Magnus theory and generic transient dynamics in periodically driven many-body quantum systems, *Ann. Phys.* **367**, 96 (2016).
- [32] T. Mori, T. Kuwahara, and K. Saito, Rigorous Bound on Energy Absorption and Generic Relaxation in Periodically Driven Quantum Systems, *Phys. Rev. Lett.* **116**, 120401 (2016).
- [33] D. Abanin, W. De Roeck, W. W. Ho *et al.*, A rigorous theory of many-body prethermalization for periodically driven and closed quantum systems, *Commun. Math. Phys.* **354**, 809 (2017).
- [34] T. Gulden, E. Berg, M. S. Rudner *et al.*, Exponentially long lifetime of universal quasi-steady states in topological Floquet pumps, *SciPost Phys.* **9**, 015 (2020).
- [35] A. Rubio-Abadal, M. Ippoliti, S. Hollerith, D. Wei, J. Rui, S. L. Sondhi, Ve. Khemani, C. Gross, and I. Bloch, Floquet Prethermalization in a Bose-Hubbard System, *Phys. Rev. X* **10**, 021044 (2020).
- [36] A. Kyprianidis, F. Machado, W. Morong *et al.*, Observation of a prethermal discrete time crystal, *Science* **372**, 1192 (2021).
- [37] P. Peng, C. Yin, X. Huang *et al.*, Floquet prethermalization in dipolar spin chains, *Nat. Phys.* **17**, 444 (2021).
- [38] A. Cao, R. Sajjad, H. Mas *et al.*, Prethermal dynamical localization and the emergence of chaos in a kicked interacting quantum gas, [arXiv:2106.09698](https://arxiv.org/abs/2106.09698).
- [39] R. Citro, E. Dalla Torre, L. DAlessio *et al.*, Dynamical stability of a many-body Kapitza pendulum, *Ann. Phys.* **360**, 694 (2015).
- [40] A. Rajak, R. Citro, and E. Dalla Torre, Stability and prethermalization in chains of classical kicked rotors, *J. Phys. A: Math. Theor.* **51**, 465001 (2018).
- [41] O. Howell, P. Weinberg, D. Sels, A. Polkovnikov, and M. Bukov, Asymptotic Prethermalization in Periodically Driven Classical Spin Chains, *Phys. Rev. Lett.* **122**, 010602 (2019).
- [42] T. Mori, Floquet prethermalization in periodically driven classical spin systems, *Phys. Rev. B* **98**, 104303 (2018).
- [43] A. Rajak, I. Dana, and E. G. Dalla Torre, Characterizations of prethermal states in periodically driven many-body systems with unbounded chaotic diffusion, *Phys. Rev. B* **100**, 100302(R) (2019).
- [44] E. G. Dalla Torre and D. Dentelski, Statistical Floquet prethermalization of the Bose-Hubbard model, *SciPost Phys.* **11**, 040 (2021).
- [45] A. Das, K. Damle, A. Dhar *et al.*, Nonlinear fluctuating hydrodynamics for the classical XXZ spin chain, *J. Stat. Phys.* **180**, 238 (2020).
- [46] A. Kundu, A. Rajak, and T. Nag, Dynamics of fluctuation correlation in periodically driven classical system, *Phys. Rev. B* **104**, 075161 (2021).
- [47] B. V. Chirikov, A universal instability of many-dimensional oscillator systems, *Phys. Rep.* **52**, 263 (1979).
- [48] K. Kaneko and T. Konishi, Diffusion in Hamiltonian dynamical systems with many degrees of freedom, *Phys. Rev. A* **40**, 6130 (1989).
- [49] T. Konishi and K. Kaneko, Diffusion in Hamiltonian chaos and its size dependence, *J. Phys. A: Math. Gen.* **23**, L715 (1990).
- [50] B. Chirikov and V. Vecheslavov, Theory of fast Arnold diffusion in many-frequency systems, *J. Stat. Phys.* **71**, 243 (1993).
- [51] M. Antoni and S. Ruffo, Clustering and relaxation in Hamiltonian long-range dynamics, *Phys. Rev. E* **52**, 2361 (1995).
- [52] M. Mulansky, K. Ahnert, A. Pikovsky *et al.*, Strong and weak chaos in weakly nonintegrable many-body Hamiltonian systems, *J. Stat. Phys.* **145**, 1256 (2011).
- [53] A. Rajak and I. Dana, Stability, isolated chaos, and superdiffusion in nonequilibrium many-body interacting systems, *Phys. Rev. E* **102**, 062120 (2020).
- [54] B. Chirikov and D. Shepelyansky, Chirikov standard map, *Scholarpedia* **3**, 3550 (2008).
- [55] B. Chirikov and V. Vecheslavov, Arnold diffusion in large systems, *J. Exp. Theor. Phys.* **85**, 616 (1997).
- [56] N. N. Nekhoroshev, An exponential estimate of stability time in Hamiltonian systems close to integrable, *Usp. Mat. Nauk* **32**, 5 (1977).
- [57] S. Choi, J. Choi, R. Landig *et al.*, Observation of discrete time-crystalline order in a disordered dipolar many-body system, *Nature (London)* **543**, 221 (2017).
- [58] A. Shapere and F. Wilczek, Classical Time Crystals, *Phys. Rev. Lett.* **109**, 160402 (2012).
- [59] N. Y. Yao, C. Nayak, L. Balents *et al.*, Classical discrete time crystals, *Nat. Phys.* **16**, 438 (2020).
- [60] A. Pizzi, A. Nunnenkamp, and J. Knolle, Classical Prethermal Phases of Matter, *Phys. Rev. Lett.* **127**, 140602 (2021).
- [61] A. Pizzi, A. Nunnenkamp, and J. Knolle, Classical approaches to prethermal discrete time crystals in one, two, and three dimensions, *Phys. Rev. B* **104**, 094308 (2021).